Electronic structure of the silicon divacancy

Osamu Sugino and Atsushi Oshiyama
Fundamental Research Laboratories, NEC Corporation, 34 Miyukigaoka, Tsukuba 305, Japan
(Received 6 July 1990)

We have calculated the electronic structure of the silicon divacancy using the self-consistent Green's-function method. We find that, for the ideal divacancy, there are two deep levels (e_g and e_u) in the band gap and that the charge state changes from V_2^{2-} to V_2^{+} as the Fermi level varies from the bottom of the conduction band to the top of the valence band. The Fermi-level dependence of the most stable charge state, i.e., the occupancy level structure, is in agreement with the experiment. We investigate the lattice relaxation of the surrounding silicon atoms by combining the electronic-structure results from the Green's-function calculation with the valence-force model, and evaluate the amount of the Jahn-Teller relaxation. We find that the relaxation is small; the Jahn-Teller energy is $\simeq 20$ meV for V_2^{+}, in reasonable agreement with the electron paramagnetic resonance experiment. Examination of the calculated results and the experimental data available leads us to conclude that the electronic level structures of the distorted divacancy are $(b_u)^1$ for V_2^{+}, $(b_u)^2$ for V_2^{0}, $(b_u)^2(a_g)^1$ for V_2^{-}, and $(b_u)^2(a_g)^2$ for V_2^{2-}, respectively. On the basis of the obtained electronic structure, we propose a new reorientation process of V_2^{-} via a metastable configuration.

I. INTRODUCTION

The silicon divacancy V_2 is one of the most fundamental defects in covalent semiconductors. It is fundamental not only because it is simple and intrinsic but also because it is easily formed by electron irradiation at room temperature.[1-13] Furthermore, the divacancy is more conveniently measured than the monovacancy or the self-interstitial silicon because, contrary to these defects, it is not mobile at room temperature owing to the large activation energy for diffusion.[1] In fact, the divacancy has long been studied by many researchers using various experimental techniques, such as electron paramagnetic resonance (EPR),[1-3] infrared (ir) spectroscopy,[8-12] photoconductivity,[11-13] and deep-level transient spectroscopy (DLTS).[4-7]

Let us summarize the experimental findings with which we are concerned in this paper. The charge state of the divacancy changes from V_2^{2-} to V_2^{+} as the Fermi level varies from the bottom of the conduction band to the top of the valence band. The existence of the charge states V_2^{-} and V_2^{+} is verified from the EPR measurements[1] and that of V_2^{2-} and V_2^{-} from the DLTS measurements.[6] The Fermi energy at which the transition between stable charge states occurs, namely, the occupancy level structure, is estimated from these two kinds of experiments; they give approximately the same level structure, although there remains a controversy as to the quantitative aspect.[6] According to the EPR study,[1] V_2^{+} and V_2^{-} have a spin $\frac{1}{2}$ and g factor close to 2. Both charge states are considered to be Jahn-Teller distorted with the reorientation activation energies between three equivalent orientations being roughly 60 meV.

To understand these characteristics a simple linear combination of atomic orbitals (LCAO) molecular-orbital model or tight-binding models have been used in most cases. Although useful for a very rough understanding, it does not offer quantitative information. In fact, the one-electron-level structure is drastically sensitive to the tight-binding parameters.[14,15] Later, Jaros and his collaborators did more elaborate calculations of the electronic level structures of the divacancy.[16,17] Yet it seems that the reliable one-electron-level structure has not been obtained, presumably due to the artificial boundary effect in the former calculation,[16] and the lack of the self-consistency in the latter calculation.[17] Moreover, the occupancy level structure and the electron-lattice coupling constant have not been investigated theoretically so far, although they are very important for interpreting the experimental data.

In this paper we report our parameter-free Green's-function calculation,[18-21] for the divacancy in silicon. The calculation is done within the local-density approximation, and the reduced-space concept[19,21] for the basis set is adopted. Lattice relaxation around the divacancy is investigated by combining the electronic-structure results from the Green's-function calculation with the lattice distortion energy from the valence-force model. The result provides us with the Jahn-Teller energy and the electronic level structure for the relaxed divacancy. On the basis of thus determined level structure, we have obtained new insight into the characteristics of the divacancy. We propose a new interpretation of the reorientation process of V_2^{-} whose activation energy was determined by EPR experiment. We also give information which may help in interpreting the ir and the photoconductivity data. In Sec. II the calculation method is briefly described, and the results are presented in Sec. III. Section IV concludes our paper.

II. METHOD OF CALCULATION

By the self-consistent Green's-function method we calculate the one-electron Green's function in which the

electron-electron interaction is self-consistently taken into account within the local-density approximation. Let us begin with the definition of the Green's matrix[19,21] expressed by a localized basis $\{\phi_\nu(\mathbf{r})\}$:

$$\sum_{\nu''}(\varepsilon S_{\nu\nu''}-H_{\nu\nu''})G_{\nu''\nu'}(\varepsilon)=\delta_{\nu\nu'} , \tag{1}$$

where $S_{\nu\nu'}$ and $H_{\nu\nu'}$ are the overlap and the Hamiltonian matrix, respectively, i.e.,

$$S_{\nu\nu'}\equiv\int d\mathbf{r}\,\phi_\nu^*(\mathbf{r})\phi_{\nu'}(\mathbf{r}) \tag{2}$$

and

$$H_{\nu\nu'}\equiv\int d\mathbf{r}\,\phi_\nu^*(\mathbf{r})[-\tfrac{1}{2}\nabla^2+\hat{V}(\mathbf{r})]\phi_{\nu'}(\mathbf{r}) . \tag{3}$$

When the eigenfunction $\Psi_i(\mathbf{r})$ of the Hamiltonian is obtained as

$$\Psi_i(\mathbf{r})=\sum_\nu c_{i\nu}\phi_\nu(\mathbf{r}) , \tag{4}$$

we can immediately construct the Green's matrix for the system as

$$G_{\nu\nu'}(\varepsilon)=\sum_i\frac{c_{i\nu}c_{i\nu'}^*}{\varepsilon-\varepsilon_i} , \tag{5}$$

where ε_i is the one-electron energy.

When a defect is introduced to the crystal, the system is perturbed by the defect-induced potential. In this case, since the system lacks periodicity, we cannot obtain $c_{i\nu}$ by the band calculation technique in which the periodicity is assumed. Instead, we evaluate the Green's function directly from Eq. (1). Or, equivalently, we can evaluate the Green's function by solving the Dyson equation,[19]

$$G_{\nu\nu'}(\varepsilon)=G^0_{\nu\nu'}(\varepsilon)+\sum_{\nu''\nu'''}G^0_{\nu\nu''}(\varepsilon)\bar{U}_{\nu''\nu'''}G_{\nu'''\nu'}(\varepsilon) , \tag{6}$$

where $G_0(\varepsilon)$ is the Green's matrix for the perfect crystal, and $\bar{U}$ consists of the defect-induced potential and the correction term, depending on the basis employed in the calculation.[19]

Using the Green's matrix, we obtain the density matrix by the following formula:

$$\rho_{\nu\nu'}=\frac{1}{2\pi i}\oint_C dz\,G_{\nu\nu'}(z) , \tag{7}$$

where the contour C encloses those poles of $G_{\nu\nu'}(z)$ corresponding to the occupied states of the system. Using the density matrix we evaluate the charge density as

$$\rho(\mathbf{r})=\sum_{\nu\nu'}\phi_\nu(\mathbf{r})\rho_{\nu\nu'}\phi_{\nu'}(\mathbf{r}) . \tag{8}$$

Using the local-density approximation we obtain the defect-induced potential again from the charge density. We repeat the procedure until the calculated perturbation becomes the same as the perturbation which is used to get $G_{\nu\nu'}$ in Eq. (6): the self-consistent solution of the Dyson equation.

In our calculation we have required self-consistency only for the valence electrons, and the core electrons are expressed by the *ab initio* pseudopotential.[22] We have used as the localized basis *s*- and *p*-type Gaussian functions centered on atom sites. The exponent of the Gaussian function is 0.18 and 0.65 for the *s*-type function and 0.15 and 0.45 for the *p*-type function in the atomic unit; thus we have used eight functions for each atom site. An inclusion of *d*-type functions (with exponent 0.18) slightly affects the one-electron-level structure of the ideal divacancy as well as the coupling of the electron with the breathing mode, which justifies the validity of our *sp* basis ste.

We have chosen a cluster of 32 sites that contains the vacant sites at the central position. The perturbation $\bar{U}$ and the Green's function are described by the basis functions in this cluster. This cluster contains the second-nearest-neighbor atoms from the vacant sites. We consider this to be large enough for the ideal divacancy because, from our experience of the Green's-function calculation,[21] the inclusion of up to the second-nearest neighbor around the perturbed sites has been found to be enough for the convergence of the electronic structures. We have also checked the convergency for relaxed divacancy: The electron-lattice coupling constants already converge with the 20-site-cluster calculation.

III. RESULTS AND DISCUSSION

A. Ideal divacancy

First let us show the electronic structure of the ideal (i.e., unrelaxed) divacancy. We have found that two localized states appear in the band gap when two Si atoms are removed from their lattice sites. They are called e_u and e_g according to the irreducible representation of the D_{3d} group, and are doubly degenerate. The energy levels for the V_2^0 charge state are shown in Fig. 1; the e_u and e_g levels appear at 0.31 and 0.64 eV, respectively, above the top of the valence band. The band gap in our calculation is 0.72 eV, considerably smaller than the experimental value, 1.17 eV. This is due to the limitation of the local-density approximation combined with the incompleteness of the basis set.

At this point we note that the extended Hückel calculation by Lee and McGill,[14] which is frequently used to interpret the experimental data, underestimates the energy of the defect level. In fact, the e_u level sinks below the valence-band top in their calculation. On the other hand, the cluster calculation of Kiron *et al.*[16] overestimated it and the a_{1u} level, which is located below the valence band in our calculation, appears in the band gap. Only

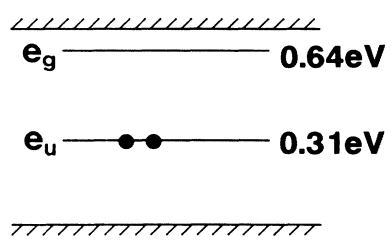

FIG. 1. Single-electron-level structure of the neutral ideal divacancy. Two electrons are accommodated in the e_u level.

Humphreys *et al.*[17] correctly showed the presence of the e_u and e_g levels in the band gap using the Green's-function calculation with a model defect potential.

These two states mainly consist of the six dangling-bond orbitals of the nearest-neighbor atoms. There is a close similarity between the wave functions of the e_u and e_g states; when we draw the contour plots of the wave functions in the plane including the three atoms nearest to one of the vacant sites, the plots are approximately the same, as shown in Fig. 2(a). It is worth noting that the wave functions of the e_u and e_g states have the nodal plane including the divacancy axis; i.e., they are both the antibonding states among the dangling-bond orbitals of the three Si atoms. The difference between the e_u and e_g states is in the change of signs of the wave function along the divacancy axis [Fig. 2(b)]; for the e_g state there is one node between the two vacancy sites and for the e_u state there is no node. Namely, the e_u and e_g are the bonding and antibonding states, respectively, of the two linear combinations, each of which consists of three dangling-bond orbitals of the Si atoms nearest to one of the two vacant sites. The separated energy of 0.33 eV (Fig. 1) is thus due to this difference.

Next we have calculated the intrasite Coulomb energy (Hubbard U) for the e_u level, which is defined as the shift of the e_u level upon accommodation of an additional electron. The result is $U=0.15$ eV for every charge state within a scattering of 0.02 eV. Upon adding the one electron to the e_u level, the e_g level also shifts upward by 0.14 eV. Since the wave functions of the e_u and e_g are similar to each other (Fig. 2), the value 0.14 eV could be regarded as the Hubbard U for the e_g level. In other words, the similarity of the wave functions of e_u and e_g results in a similar response to the addition of an electron.

Finally, we mention the occupancy level structure. To calculate it we have to compare the difference of the free energy when an electron at the Fermi level μ is brought to the defect level which has been occupied by N electrons, i.e., $\Delta G=E(N+1)-E(N)-\mu$. We have evaluated the total energy difference using Slater's argument. We show in Fig. 3 the occupancy level structure obtained. The most stable charge state changes from V_2^{2-} to V_2^{+} as the Fermi level varies from the bottom of the conduction band to the top of the valence band. The existence of the four charge states, together with the transition energy between different charge states, is consistent with the experiment. This seems to show that the effect of the lattice relaxation is not so large as to change the occupancy level structure from that of the ideal divacancy.

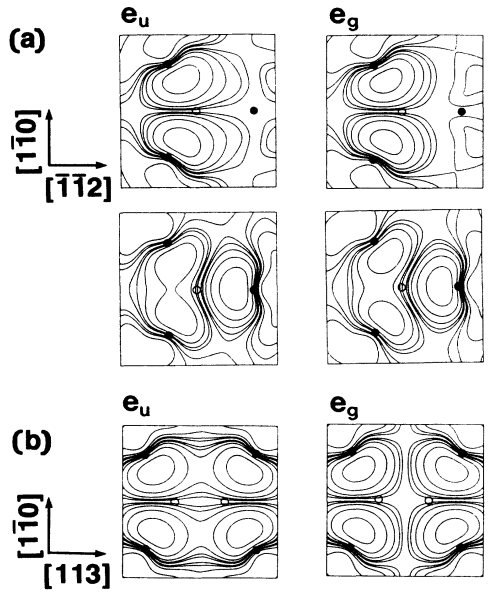

FIG. 2. Wave functions for the e_u state and the e_g state. (a) Contour plots in the plane including the three atoms nearest one of the vacant sites. Upon Jahn-Teller distortion the lower (upper) of the e_u states changes continuously to the b_u (a_u) state, and the lower (upper) one of the e_g states to the changed a_g (b_g) state. The maximum value of the plot is 5.0×10^{-2} (electrons)$^{1/2}$(a.u.)$^{-3/2}$, and the subsequent contour lines differ by a factor of 2. (b) Contour plots in the plane including four of the six nearest-neighbor atoms. In these figures the closed circles correspond to the position of the atom and the open circles correspond to the vacancy site (the vacancy sites are not on the plane).

B. Lattice relaxation

Now we consider the lattice relaxation. Instead of calculating the relaxation from first principles, we semiquantitatively evaluate the amount of relaxation using a model in which the electronic-structure results from the Green's function are combined with the lattice distortion energy from the valence-force model. In this model the total energy is expanded quadratically with the normal mode Q,

$$E(N,Q)=E(N,Q=0)-NVQ+\tfrac{1}{2}kQ^2\ , \tag{9}$$

where N is the number of electrons in the defect level and the force constant k is determined by the valence-force

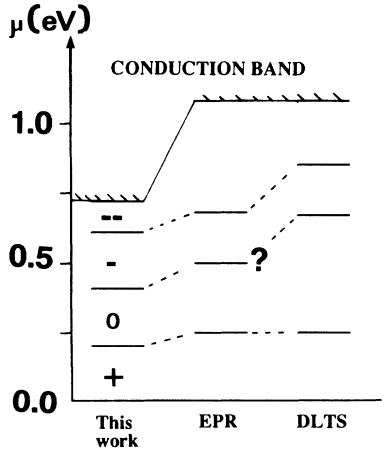

FIG. 3. Occupancy level structure of the ideal divacancy. For comparison with the experiments we show the occupancy level structure deduced from the EPR data of Watkins and Corbett (Ref. 1) and that deduced from the DLTS data by Evwaraye and Sun (Ref. 6).

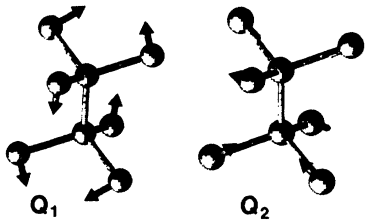

FIG. 4. Normal modes of the Jahn-Teller distortion (Q_1 and Q_2) that lower the symmetry from D_{3d} to C_{2h}.

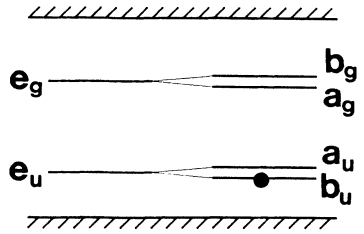

FIG. 5. Electronic-level structure of the Jahn-Teller-distorted positively charged divacancy.

model. The electron-lattice coupling constant V is determined from the variation of the relevant single-electron level with increasing Q. The amount of the distortion and the energy gain (cost) for that distortion are determined by minimizing this formula. This method is essentially identical to that used by Baraff *et al.* for silicon monovacancy.[23]

The divacancy is known to undergo the breathing distortions of the neighboring atoms that keep the D_{3d} symmetry and the Jahn-Teller distortions that lower the symmetry to C_{2h}. Since, according to our preliminary local-density calculation for the supercell geometry, the breathing distortion is not significant, we consider only the Jahn-Teller distortion here. There are two independent Jahn-Teller modes Q_1 and Q_2, which are shown in Fig. 4. We have considered both modes in this paper.

First we calculate the splitting of the e_u level upon the symmetry-lowering distortion Q_1 and Q_2 by the Green's-function calculation. The amount of the splitting depends, in principle, on the charge state. This may be unimportant in the present case, however. We thus obtain V_1 and V_2 shown in Table I. As for the force constant, we use the valence-force model[24] in which long-range relaxation up to 18 shells of Si atoms around the divacancy is taken into account. The results are also listed in Table I. We have to note here that the k is very sensitive to the parameters used and thus we have to consider that the result is only qualitative. In fact, if we use the parameter adopted by Baraff *et al.*[23] instead of that adopted by Martins,[24] we obtain k's that are less than half of the k in Table I. In this case the amount of the distortion and the Jahn-Teller energy E_{JT} is more than twice larger.

For V_2^+ we have obtained the amount of the distortion as $Q_1=0.00$ Å, virtually no relaxation, and $Q_2=0.08$ Å and E_{JT} as 20 meV for the second mode Q_2. This is consistent with the EPR experiment of Watkins and Corbett.[1] According to them the activation energy for reorientation between three equivalent distortions is 73 meV for V_2^+. For V_2^0, as can be shown from Eq. (9), the amount of the distortion and E_{JT} are, respectively, two and four times compared with V_2^+. For other charge states things are more complicated and will be discussed in Sec. III C.

Since the relaxation along the first mode is negligibly small, we discuss only the second mode hereafter. Upon the Jahn-Teller relaxation the energy level e_u splits into the b_u and a_u levels and the e_g level splits into the a_g and b_g levels as shown in Fig. 5. As to the wave function, the lower (upper) of the e_u states which is shown in Fig. 2(a) continuously changes to the wave function of the b_u (a_u) state. Similarly, the lower (upper) of e_g states in Fig. 2(a) continuously changes to the wave function of the a_g (b_g) state.

The electronic structure is thus $(b_u)^1$ for V_2^+ and $(b_u)^2$ for V_2^0. This level structure is different from that supposed by Watkins and Corbett.[1] They suggested $(a_g)^1$ for V_2^+ and $(a_g)^2$ for V_2^0. The level structure of Watkins and Corbett seems to be inconsistent with their own experiment because, in order for the Jahn-Teller distortion to be large enough to reverse the energy-level scheme from that of Fig. 5, the E_{JT} have to be larger than the splitting of the e_u and e_g levels, 330 meV. Further, in that case, the Jahn-Teller energy, which is proportional to the square of the number of electrons in the defect level, for more negative charge states becomes much larger than U. This may result in the unstable V_2^0, V_2^-, and V_2^{2-}.

TABLE I. Calculated parameters V (eV/Å) and k (eV/Å^2). k is obtained by the valence-force model calculation adopting the parameter of Martin (Ref. 24).

$$\begin{bmatrix} V_1 \\ V_2 \end{bmatrix} = \begin{bmatrix} 0.1 \\ -0.6 \end{bmatrix} \qquad k_{ij} = \begin{bmatrix} 4.3 & -0.19 \\ -0.19 & 7.5 \end{bmatrix}$$

C. Energy-level structure of V_2^- and V_2^{2-}

The energy-level structure of V_2^-, V_2^{2-} is rather complicated and it needs a cautious treatment. First, we naively construct the level structure for V_2^-. Since the b_u state is already fully occupied for V_2^0, the third electron occupies the next higher level a_u to make V_2^-. In this case, since the derivative of the energy level of the a_u with respect to Q, i.e., V_{a_u}, is positive, the Jahn-Teller distortion is reduced. If $V_{a_u} \simeq V_{b_u}$ holds, as is expected from a perturbational sense, a partial cancellation occurs and the Jahn-Teller relaxation is effectively caused by one of the two electrons in the b_u state. As a result, E_{JT} is approximately the same as that for V_2^+.

However, another level structure is realized when the energy separation between the a_u and a_g in Fig. 5 is smaller compared with the Jahn-Teller energy gain by ex-

citing the third electron from the Jahn-Teller decelerating state a_u to the Jahn-Teller accelerating state a_g, and further distortion is thus accomplished. In this case the energy-level structure is $(b_u)^2(a_g)^1$ rather than $(b_u)^2(a_u)^1$. This occurs for sufficiently small k because the energy gain by Jahn-Teller distortion is easier for smaller k. Roughly estimating, this crossover occurs when the k is less than half the value of k in Table I. Thus we are unable to decide which is indeed realized solely from the present semiquantitative model. So let us refer to the existing experimental data.

Ammerlaan and co-workers[4] have investigated the wave function of the unpaired electron accommodated in the localized defect level for V_2^+ and V_2^- using the electron-nucleus double resonance (ENDOR) technique. They probed the wave function at more than 100 sites, and they concluded that the wave functions of both charge states are very similar to each other, except that its extent is somewhat larger for V_2^-. They also showed that the $3s$ component of the wave function has a maximum amplitude at the two nearest-neighbor atom sites which are in the mirror plane of the C_{2h} configuration, i.e., the atom sites on the right-hand side in Fig. 2(a). From this result the wave function cannot be the b_g or a_u because, from the symmetry consideration, they have a node at the above-mentioned mirror plane site and thus the wave function has no $3s$ component, as shown in Fig. 2(a). Therefore the electronic-level structure is $(b_u)^2(a_g)^1$ rather than $(b_u)^2(a_u)^1$.

This electronic structure is also consistent with the EPR experiment by Watkins and Corbett,[1] in which the activation energy for reorientation between three equivalent distortions is 56 meV for V_2^-. For V_2^- we argue that the reorientation process is somewhat more complicated than that for V_2^+. In the reorientation process of V_2^-, the electronic-level structure changes from that of the ground state, $(b_u)^2(a_g)^1$, to that of the metastable state, $(b_u)^2(a_u)^1$, in the first place. Then the metastable state reorients itself to one of its three quivalent distorted states. Finally it returns to the ground state. The whole process is drawn conceptually in Fig. 6. Roughly estimating with the assumption that $V_{a_u} \simeq -V_{b_u}$ and $V_{b_u} \simeq V_{a_g}$, the activation energy for the second process is the largest and it is approximately the same as the reorientation activation energy for V_2^+. This is consistent with the experimental fact that the activation energy for the reorientation is roughly the same for both charge states.

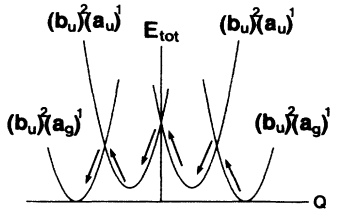

FIG. 6. Conceptual picture of the reorientation process of the V_2^-.

The electronic-level structure for V_2^{2-} will then be $(b_u)^2(a_g)^2$. Since the Jahn-Teller energy gain is proportional to N^2, the relaxation energy gain is much larger than that of V_2^-, resulting in a tendency to occupy the a_g level.

Finally we give a comment as to the not yet settled assignment of the ir and photoconductivity spectrum. We have shown that very similar wave functions were observed for V_2^+ and V_2^- in the ENDOR experiment.[3] According to above-mentioned level structure, this means that there is a similarity of wave function for the two levels b_u and a_g, which we have incidentally found from our calculation (Fig. 2). In general, the similarity of the wave function gives rise to a similar response to the perturbation. This means that the both b_u level and a_g level respond to the Jahn-Teller distsortion in approximately the same manner. As a result, the transition $b_u \rightarrow a_g$ is not accompanied by a large change in the Jahn-Teller distortion. However, in assigning the ir spectra, it has been frequently assumed that the Jahn-Teller distortion in the excited state is substantially different from that in the ground state, and some candidates for the assignment have been thus discarded.[3] We suggest here that excitation without a large change in the Jahn-Teller distortion should be observed.

To confirm the above-mentioned considerations theoretically, we have to calculate the *ab initio* Green's-function calculation for fully distorted divacancy and determine level structures, wave functions, and the occupancy level structure. We consider it to be a subtle problem to determine which configuration gives a lower total energy for V_2^- from first principles: e.g., the Green's-function calculation with the more complete basis set will be desirable. Moreover, it is necessary to determine the amount of relaxation unambiguously. To give quantitative information about the photospectrum, we will have to overcome the difficulty associated with the local-density approximation. In this way there are still many points yet to be clarified.

IV. CONCLUSION

We have calculated the electronic structure of the silicon divacancy using the self-consistent Green's-function method. We find that, for the ideal divacancy, there are two deep levels (the e_g and e_u) in the band gap and that the charge state changes from V_2^{2-} to V_2^+ as the Fermi level varies from the bottom of the conduction band to the top of the valence band. The Fermi-level dependence of the stablest charge state is in agreement with experiment, which suggests that the effect of the neighboring lattice distortion is not so large as to change the occupancy level structure from that of the ideal divacancy. We have indeed calculated the amount of the Jahn-Teller distortion with the aid of the valence-force model. We find that the Jahn-Teller relaxation is small; E_{JT} is 20 meV for V_2^+ and 80 meV for V_2^0. For the four charge states we have determined the electronic-level structure as $(b_u)^2$ for V_2^+, $(b_u)^2$ for V_2^0, $(b_u)^2(a_g)^1$ for V_2^-, and $(b_u)^2(a_g)^2$ for V_2^{2-}, by combining the present results with the

ENDOR data. On this basis we have suggested a new reorientation process for V_2^-. We have also found that the wave functions of the b_u state and the a_g state are very similar to each other, which suggests that the transition $b_u \rightarrow a_g$ is not accompanied by a large change in the Jahn-Teller distortion. This may help in assigning the ir and photoconductivity spectra, which is still controversial.

[1]G. D. Watkins and J. W. Corbett, Phys. Rev. **138**, A543 (1965).
[2]J. W. Corbett and G. D. Watkins, Phys. Rev. **138**, A555 (1965).
[3]C. A. J. Ammerlaan and G. D. Watkins, Phys. Rev. B **5**, 3988 (1972).
[4]E. G. Sieverts, S. H. Muller, and C. A. J. Ammerlaan, Phys. Rev. B **18**, 6834 (1978); J. G. de Wit, E. G. Sieverts, and C. A. J. Ammerlaan, *ibid.* **14**, 3494 (1976).
[5]B. G. Svensson and M. Willander, J. Appl. Phys. **62**, 2758 (1987).
[6]A. O. Evwaraye and E. Sun, J. Appl. Phys. **47**, 3776 (1976).
[7]G. A. Samara, Phys. Rev. B **39**, 12764 (1989).
[8]L. J. Cheng, J. C. Corelli, J. W. Corbett, and G. D. Watkins, Phys. Rev. **152**, 761 (1966).
[9]L. J. Cheng and P. Vajada, Phys. Rev. **186**, 816 (1969).
[10]C. S. Cheng and J. C. Corelli, Phys. Rev. B **5**, 1505 (1972).
[11]R. C. Young and J. C. Corelli, Phys. Rev. B **5**, 1455 (1972).
[12]H. Y. Fan and A K. Ramdas, J. Appl. Phys. **30**, 1127 (1959).
[13]C. E. Barnes, Radiat. Eff. **8**, 221 (1971).
[14]T. F. Lee and T. C. McGill, J. Phys. C **6**, 3438 (1973).
[15]E. Kauffer, P. Pécheur, and M. Gerl, Rev. Phys. Appl. **15**, 849 (1980).
[16]M. J. Kirton, P. W. Banks, Lu. Da. Lian, and M. Jaros, J. Phys. C **17**, 2487 (1984).
[17]R. G. Humphreys, S. Brand, and M. Jaros, J. Phys. C **16**, L337 (1983).
[18]J. Bernholc, N. O. Lipari, and S. T. Pantelides, Phys. Rev. Lett. **41**, 895 (1978); Phys. Rev. B **21**, 3545 (1980).
[19]A. R. Williams, P. J. Feibelman, and N. D. Lang, Phys. Rev. B **26**, 5443 (1982).
[20]G. A. Baraff and M. Schlüter, Phys. Rev. Lett. **41**, 892 (1978).
[21]R. Car, P. J. Kelly, A. Oshiyama, and S. T. Pantelides, Phys. Rev. Lett. **52**, 1814 (1984).
[22]G. B. Bachelet, D. R. Hamann, M. Schlüter, Phys. Rev. B **26**, 4199 (1982); D. R. Hamann, M. Schlüter, and C. Chiang, Phys. Rev. Lett. **43**, 1494 (1979).
[23]G. A. Baraff, E. O. Kane, and M. Schlüter, Phys. Rev. B **21**, 5662 (1980).
[24]R. M. Martin, Phys. Rev. B **1**, 4005 (1970).